Electronic Supplementary Material (ESI) for Chemical Communications

Supporting information

Triggered-release in Lipid Bilayer-Capped Mesoporous Silica Nanoparticles containing SPION using an Alternating Magnetic Field

Eugenio Bringas, Özcan Köysüren, Dat V. Quach, Morteza Mahmoudi, Elena Aznar, John D. Roehling, M. Dolores Marcos, Ramón Martínez-Máñez,* and Pieter Stroeve**

Chemicals

The chemicals iron(III) chloride hexahydrate 97% ($FeCl_3 \cdot 6H_2O$), iron(II) chloride tetrahydrate 99% ($FeCl_2 \cdot 4H_2O$), ammonium hydroxide 28% NH_3 (NH_4OH), tetramethylammonium hydroxide 25% (TMAOH), tetraethylorthosilicate (TEOS), hexadecyltrimethylammonium bromide (CTAB), methylene blue ($C_{16}H_{18}ClN_3S \cdot 3H_2O$), phosphate buffer saline (PBS), 1,2-Dioleoyl-sn-glycero-3-phosphocholine ($C_{44}H_{84}NO_8P$), analytical-grade chloroform and sodium dodecyl sulfate (SDS) were provided by Sigma-Aldrich. All reagents were used as received. High quality nitrogen gas was employed to create a non-oxidizing atmosphere. For cell culture experiments, MTT (3-(4,5-dimethylthiazol-2-yl)-2,5-diphenyltetrazolium bromide), XTT (sodium(2,3-bis(2-methoxy-4-nitro-5-sulphophenyl)-2H-tetrazolium-5-carboxanilide), cell culture mediums, glutamax, antibiotic-antimycotic, non-essential aminoacids, and sodium pyruvate, propidium iodide (PI) and Triton X-100 were provided by Sigma-Aldrich.

General Techniques

Powder XRD, scanning electron microscopy (SEM) with energy-dispersive X-ray analysis (EDS), transmission electron microscopy (TEM), scanning transmission electron microscopy (STEM), and magnetic susceptibility obtained with a vibrating sample magnetometer (VSM) were used to characterize the prepared materials. X-ray measurements were performed on a Scintag EDS 2000 diffractometer using Cu-K_α radiation. SEM images were obtained with a Philips XL30-SFEG high resolution scanning electron microscope with energy-dispersive X-ray spectroscopy (EDS) capability. STEM images were

taken with a JEOL 2100F aberration corrected microscope working at 200 kV. The sample for STEM characterization was prepared by drip coating suspensions of the particles onto lacey carbon grids. The magnetization of the samples in a variable magnetic field was measured using a VSM MicroMag 2900/3900 with a sensitivity of 10^{-3} emu and a maximum magnetic field of 10 kOe. The dye release was evaluated by UV-visible spectroscopy using a Varian Cary 50 UV/Vis Spectrophotometer (Agilent Technologies). In the cytotoxicity assays the absorbance of each well, which assesses viable cells, in MTT and XTT assays were read on a microplate reader (Stat Fax-2100, AWARENESS, Palm City, USA). The results were statistically processed for outlier detection using a "T procedure" in the MINITAB software (Minitab Inc., State College, PA). Statistical differentiations were made by one-way analyses of variance (ANOVA), for which $p < 0.05$ was considered as statistically significant. For the cell cycle assays, the PI-stained cells were analyzed by flow cytometry using Cyflow SL machine (Partec, Germany) with excitation at 488 nm and collecting data at FL2. The readings were analyzed with Flowjo software (Treestar Inc., CA, USA).

Synthesis of materials

Figure SI-1 summarizes the different steps followed in the synthesis of solids **S1** and **S2**.

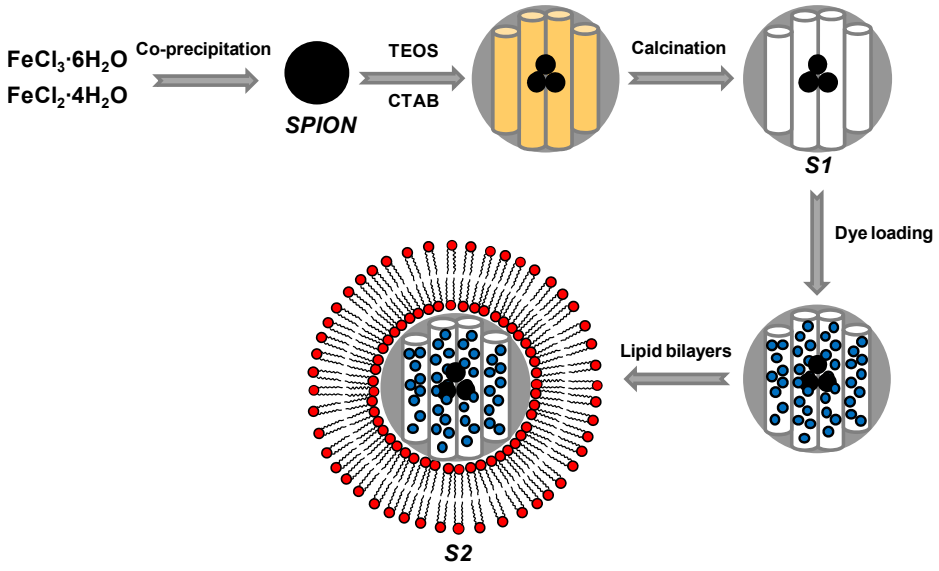

Figure SI-1.Synthesis of solids **S1** and **S2**.

a) Synthesis of superparamagnetic iron oxide NPs (SPION)

SPION were synthesized by a co-precipitation method[1] which can be summarized as follows: iron(III) chloride hexahydrate ($FeCl_3.6H_2O$, 10.81 g, 40 mmol) and iron(II) chloride tetrahydrate ($FeCl_2.4H_2O$, 3.97, 20 mmol) were first dissolved in 40 mL of degasified deionized water (DI) and 10 mL of HCl 2.00 mol L^{-1}. Then, the mixture of iron chlorides was poured drop-wise in a round bottom flask reactor containing 500 mL of a NH_4OH 0.7 mol L^{-1}. The co-precipitation reaction continued for 30 minutes at room temperature and under stirring conditions in a N_2 atmosphere to give a dark brown-black precipitate. The particles were settled down using a neodymium magnet being the supernatant removed. Finally, 60 mL of a 1 mol L^{-1} TMAOH solution was added to avoid particle agglomeration and the volume of the final ferrofluid was adjusted to 320 mL with degasified DI water. The basic ferrofluid was stored at 4°C under N_2 atmosphere.

b) Synthesis of **S1**

To synthesize the magnetic solid **S1**, hexadecyltrimethylammonium bromide (CTAB, 1.00 g, 2.74 mmol) was first dissolved in 480 mL of deionized water. Then, 30 mL of the basic ferrofluid previously synthesized (pH≈13) was added followed by an adjustment of the temperature to 80ºC. TEOS (5.00 mL, 22.4 mmol) was then added dropwise to the suspension. The mixture was stirred for 1 hour to give a brown-reddish precipitate. Finally the solid was collected by centrifugation, washed with deionized water and dried at 70ºC overnight. To prepare the final mesoporous material **S1**, the as-synthesized solid was calcined at 550 ºC using an oxidant atmosphere during 8 hours (a temperature ramp rate of 3°C/min was set during the first three hours) to remove the template.

c) Synthesis of **S2**

A certain amount of solid **S1** was dispersed in a solution of methylene blue in DI water with a mass ratio dye/solid=0.2-0.6. The mixture was initially sonicated and stirred for 24 hours. The final blue solid can be filtered off, slightly washed with DI water and dried under vacuum at 80°C overnight or

can be used wet. In a second step the loaded solid was covered by lipid bilayer by the following procedure: the phospholipid 1,2-dioleoyl-*sn*-glycero-3-phosphocholine ($C_{44}H_{84}NO_8P$, 6.6 mg, 9 μm) was first dissolved in 1.5 mL of chloroform using a precleaned glass vial. Chloroform was carefully evaporated with a small N_2 stream allowing the even distribution of the lipid on the walls of the vial after drying. 3 mL of PBS 0.25X (pH=7.4, phosphate concentration $2.5x10^{-3}$ mol L^{-1}) solution was added to the vial to redisperse the lipid. The lipid solution was sonicated with an ultrasonic tip (1/8 in. diameter; 10 W output) during two pulsed periods of 15 seconds.[2] Then, 100 μL of the vesicle solution was vigorously mixed with 25 μL of a suspension of the loaded solid (50 mg) in 5 mL of a saturated solution of methylene blue. The hybrid lipid-coated iron oxide-containing silica nanoparticles were separated by centrifugation (6000 rpm, 5 min) thanks to their high density (recovery 99%) and washed ten times with PBS 0.25x solution to obtain the final solid **S2**.

Release experiments

Solid **S2** was used as soon as it was synthesized to evaluate dye release both in the presence and in the absence of an alternating magnetic field (AMF). Two different samples were prepared by dispersing the solid **S2** in 5 mL of PBS 0.25x solution. One glass vial was exposed to an AMF while the other was taken as control. To eliminate any thermal effects from the magnet, the glass vials exposed to AMF were immersed in a water bath maintained at 21±1 °C (Figure SI-2). The AC magnet (Model No DA-604220-110AC, Magnetic Corp.) generated an oscillating magnetic field at a frequency of 50 Hz and a magnitude of 1570 G. After a fixed time, the suspension was filtered off using 0.22 μm PTFE filters and the released cargo was monitored through the monitorization of the UV-vis absorption of methylene blue at 655nm.

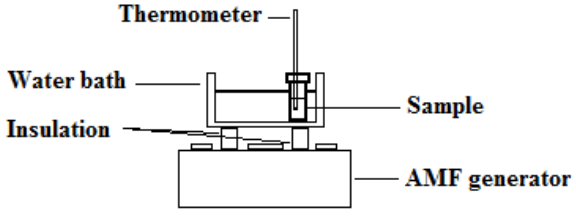

Figure SI-2.Scheme of the release experiments using **S2**.

Materials Characterization

SPION were characterized by powder XRD, SEM and VSM analysis. Figure S1-3 shows powder X-ray diffraction (XRD) pattern (a) and SEM micrographs (b) of SPION.

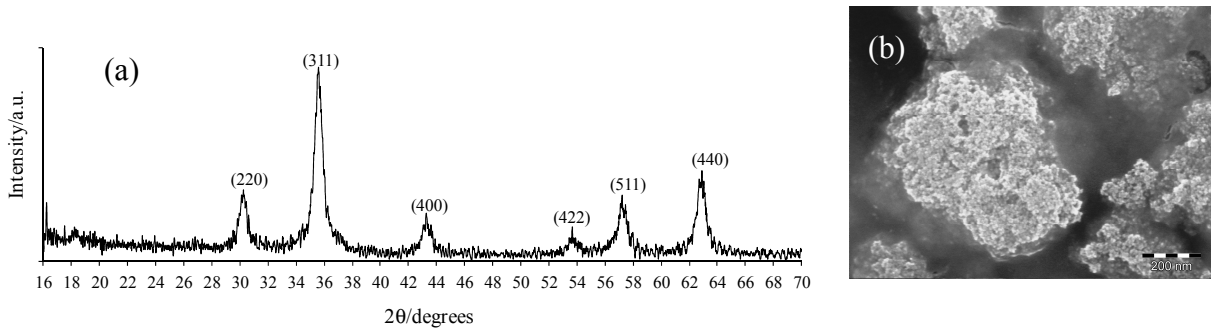

Figure SI-3. Powder X-ray diffraction patterns (a) and SEM micrographs (b) of SPION (size bar: 200 nm).

XRD reflections in Figure SI-3a can be indexed as typical Bragg peaks of a cubic array of superparamagnetic iron oxide.[3] Sen et al.[4] reported that SPION obtained by precipitation from Fe^{2+} and Fe^{3+} chloride solution and using TMAOH as dispersing agent are spherical and have an average diameter between 10 and 35 nm. Assuming spherical particles, the average diameter (d) of the SPION can be estimated by the Scherrer's formula valid for crystal sizes lower than 100 nm:

$$d = \frac{4}{3} \cdot < D >= \frac{4}{3} \cdot \frac{K \cdot \lambda}{B \cdot \cos\theta} \qquad \text{(SI-1)}$$

where <D> (nm) is the volume weighted crystallite size, K is the Scherrer constant (≈0.9), λ (nm) is the wavelength of the radiation (1.5418 Å), B is the integral breadth of a reflection located at 2θ (rad) and θ (rad) is the half of the reflection angle. The average diameter of the SPION calculated with Equation SI-1 was 18.6±0.7 nm which is within the range of the previous reported values.

From the SEM results depicted in Figure SI-3b it can be observed that SPION form agglomerates bigger than 1 μm when they are obtained as a solid powder. Nevertheless, slight agglomeration effects are expected when SPION are suspended in the ferrofluid.

Solid **S1** was characterized using standard procedures. Figure SI-4 shows low and high angle powder X-ray diffraction patterns of both the as synthesized magnetic mesoporous material (curve a) and the final

S1 material obtained after calcination (curve b). The low angle powder XRD pattern of the as-synthesized magnetic mesoporous material (curve a) shows four low-angle reflections typical of a hexagonal array that can be indexed as (100), (110), (200) and (210) Bragg peaks. A significant displacement of the (100) peak in the powder XRD of the solid **S1** is clearly appreciated in curve b, corresponding to an approximate cell contraction of 8 Å. This displacement and the broadening of the (110) and (200) peaks are related to further condensation of silanol groups during the calcination step. On the other hand, the high angle XRD pattern of material **S1** was similar to the diffraction pattern of SPION depicted in Figure SI-3.

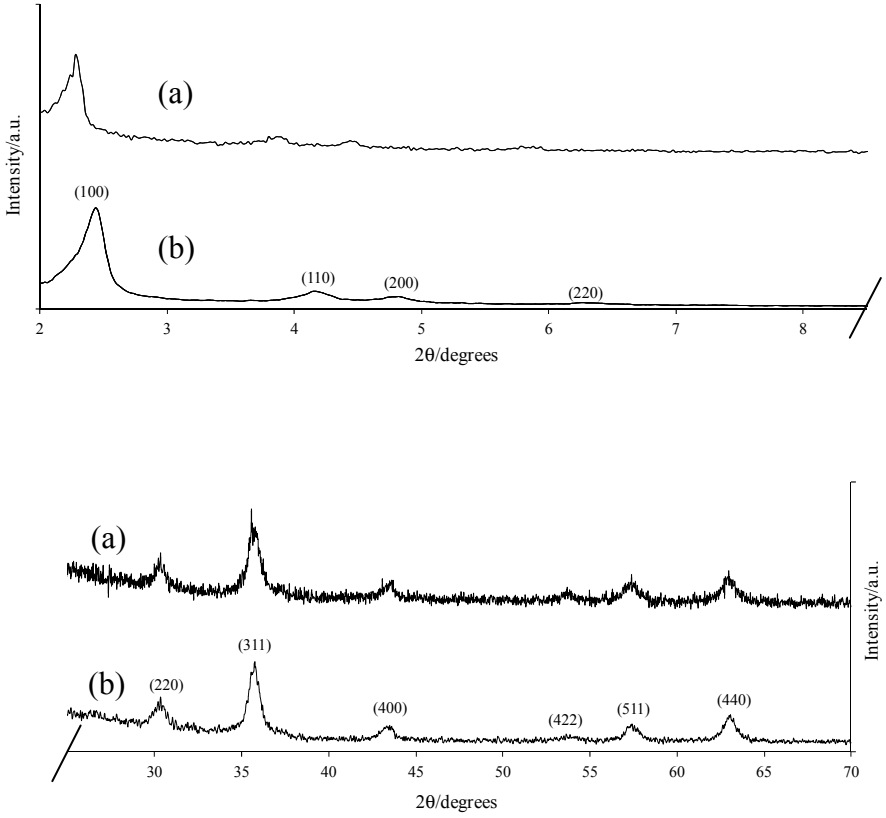

Figure SI-4. Low and high angle powder X-ray diffraction patterns of the solids (a) as-synthesized magnetic mesoporous material as-synthesized (b) solid **S1** obtained after calcination.

Figure SI-5 shows SEM (a), TEM (b) and STEM (c) images of solid **S1**. Although some agglomerates are detected due to the magnetic behavior of the solids (see Figure SI-5a), all the images evidence the almost spherical morphology of the particles and their average diameter around 100 nm. In addition, the typical

hexagonal porosity of MCM-41 mesoporous material can be observed in the silica shell which contains pores with diameters smaller than 4 nm. Moreover, the diameter of the magnetic NPs obtained from TEM images is in good agreement with the value calculated above from the XRD analysis of SPION. From TEM (Figure SI-5b) and STEM (Figure SI-5c) results it can be concluded that a combination of single core and multiple-core NPs are obtained under the selected synthesis conditions. From the EDS analysis of solid **S1** the mol ratio between silica and iron was calculated to be 4.0±0.5, this value being close to the theoretical Si/Fe mol ratio = 5.0 expected from the initial mass of TEOS and ferrofluid used in the synthesis of the magnetic NPs.

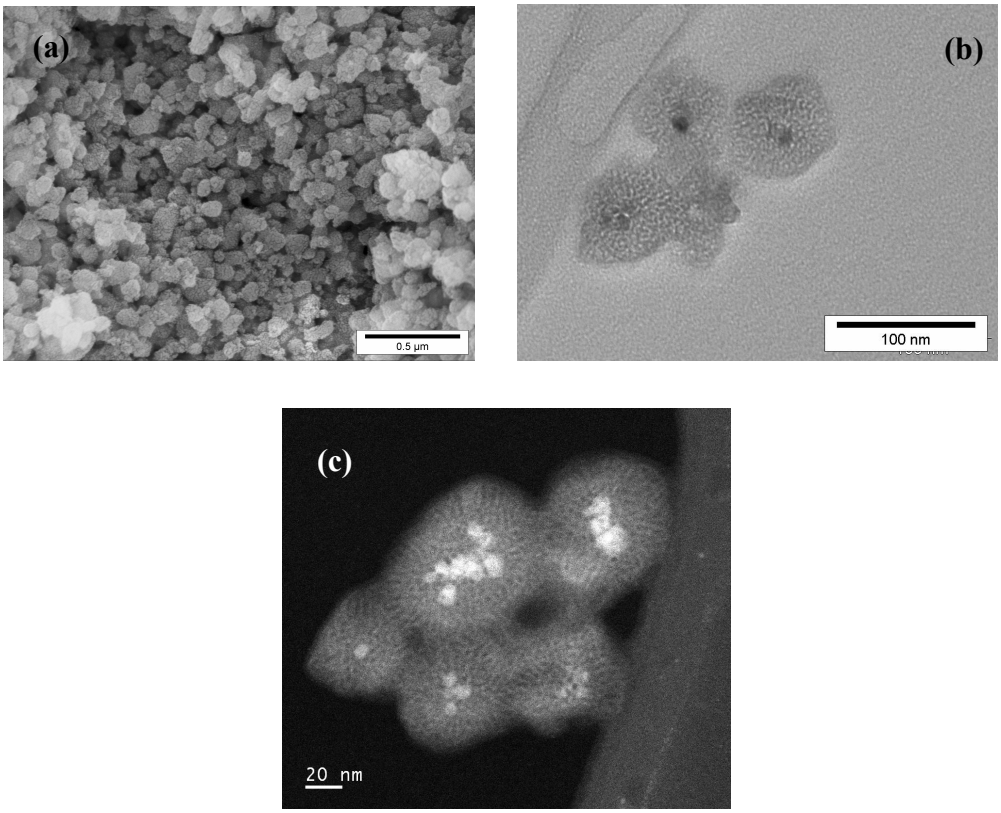

Figure SI-5.SEM (a), TEM (b) and STEM (c) of solid **S1**.

Magnetic susceptibility of SPION (Figure SI-6a) and solid **S1** (Figure SI-6b) was evaluated at 298 K using a vibrating sample magnetometer (VSM). SPION and **S1** NPs have magnetization saturation values of 52.8 and 14.0 emu/g, respectively. It should be noticed that the saturation value of iron oxide particles is four times higher than the value obtained for the composites **S1** as expected from the molar ratio between silica and iron reported above. Low coercivity values of 8.4 Oe (SPION) and 4.4 Oe (solid **S1**)

are calculated from the magnified hysteresis loops inserted in Figures SI-6a and SI-6b confirming the superparamagnetic properties of the synthesized materials. These values are in good agreement with those reported Ma et al.[5] for SPION with similar diameters.

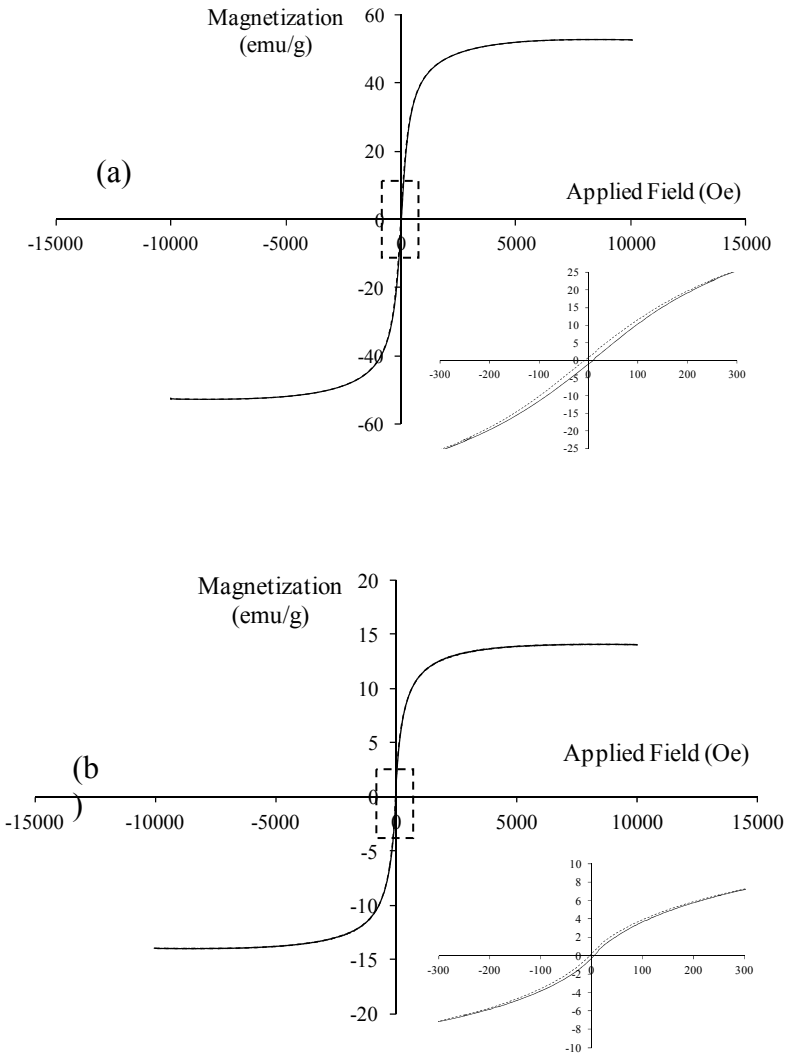

Figure SI-6.Magnetization curves of SPION (a) and solid **S1** (b).

Influence of temperature in lipid bilayer permeability

Two samples of solid S2 were dispersed in PBS (pH=7.4). One batch was stirred at 25 ºC for 45 min. After this time, the suspension was centrifuged and the released cargo was determined through the monitorization of the UV-vis absorbance band in the aqueous phase of the dye methylene blue at 655 nm. The experiment was repeated but stirring the suspension at 50 ºC for 45 min. Figure SI-7 shows the absorbance spectrum of the delivered dye in each experiment. Thus, a massive dye delivery at 50 ºC can

be observed, while the release found at 25 ºC was negligible. These results confirm the influence of temperature in the lipid bilayer permeability.

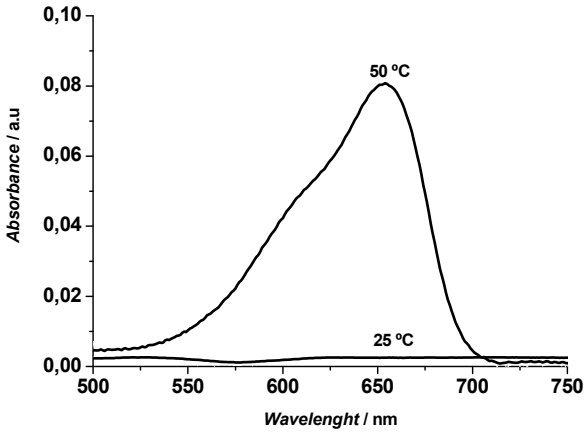

Figure SI-7. Absorbance spectrum of the delivered dye at 25 and 50ºC.

Cytotoxicity assays

The phenomenon, which is called "cell vision", is related to the fact that the defense mechanism of the cells against a foreign element could be considerably different according to the cell types. Thus, what the cell "sees", when it is faced with NPs is dependent on the cell type. In order to study the cell "vision" phenomenon effects of direct contact of solid **S2** with ten types of human cell lines were investigated using MTT and XTT procedures.[6] Another cellular process of interest is cell cycle that could adversely be affected by NPs treatments. Cell cycles were studied in the presence of **S2** using human erythromyeloblastoid leukemia cells.[7]

a) MTT and XTT assays

MTT and XTT reductions were employed to quantify metabolically active cells after exposure to the solid **S2**. All cell lines (see Table SI-2) were seeded into a 96 well-plate at a density of 10000 cells (2500 cells for Human Cardiac Myocytes (HCM)) per well in 100 µL of medium. After 24 hours, 40 µL of the corresponding suspension containing various concentrations of solid **S2** (0.25, 0.5, 1, 2, and 4 mg mL^{-1}) was added to each well. 40 µL of base medium for each cell line was added to negative control wells. All specimens as well as controls were placed in 5 wells to provide statistically reliable

results. The cells were cultured in their specific mediums (see Table SI-2) and maintained at 37°C in a 5% and 10% CO_2 incubator.

Table SI-2. Description of the cell lines used in MTT and XTT studies (DMEM: Dulbecco's Modified Eagle's Medium; Ham's: Nutrient Mixture F-10; FBS: Fetal Bovine Serum; RPMI-1640 (Roswell Park Memorial Institute))

Cell Code	Cell Type	Culture Medium
BE(2)-C	Human neuroblastoma	1:1 (DMEM + Ham's F12) + FBS10%
A172	Human glioblastoma	DMEM+FBS10%
HCM	Human cardiac myocytes	1:1 (DMEM + Ham's F12) + FBS10% supplemented with 5 µg mL^{-1} Insulin and 50 ng mL^{-1} bFGF
A549	Human lung adenocarcinoma	DMEM + FBS10%
HEP G2	Human hepatocellular carcinoma	RPMI 1640 + FBS10%
A-431	Human epithelial carcinoma	DMEM + FBS10%
293T	Human Embryonic Kidney	RPMI 1640 + FBS10%
SW480	Human colon adenocarcinoma	DMEM + FBS10%
K-562	Human erythromyeloblastoid leukemia	DMEM + FBS10%

Cytotoxicity was assessed using the MTT (3-(4,5-dimethylthiazol-2-yl)-2,5-diphenyltetrazolium bromide) and XTT (sodium(2,3-bis(2-methoxy-4-nitro-5-sulphophenyl)-2H-tetrazolium-5-carboxanilide) assays, which are non-radioactive colorimetric techniques. Considering the MTT assay, 4 and 24 hours after the incubation with solid **S2**, 100 µL of MTT (0.5 mg mL^{-1}) was added to each well. Following incubation, the medium was removed and formazan crystals were solubilized by incubation for 20 min in 150 µL of isopropanol. The absorbance of each well, which assesses viable cells, was read at 545 nm on a microplate reader. Regarding XTT assay, 4 and 24 hrs after the incubation with solid **S2**, 50 µL of XTT labeling mixture was added to each well and incubated for 18 hrs, after that the amount of formazan crystals were measured using the plate reader. For the MTT and XTT studies, all experiments were carried out in triplicate with the results expressed as mean ± standard deviation; standard deviation values are indicated as error bars in the relevant MTT plots. The

results were statistically processed for outlier detection using a "T procedure" in the MINITAB software (Minitab Inc., State College, PA).[8] Statistical differentiations were made by one-way analyses of variance (ANOVA), for which $p < 0.05$ was considered as statistically significant.

According to the results depicted in Figures SI-8 to SI-11, the toxicity of solid **S2** at concentrations lower than 0.5 mg mL^{-1} was negligible for all the cell lines under study. However, at higher concentrations (from 1 to 4 mg mL^{-1}) a trace of toxicity was observed for some of the cell lines including brain, nervous, lung, and heart extracted human cells. These small toxicity amounts are happened for some cell lines due to the fact that the brain, nervous system, lung, and heart cell lines are more sensitive to foreign materials in comparison to the other organs.

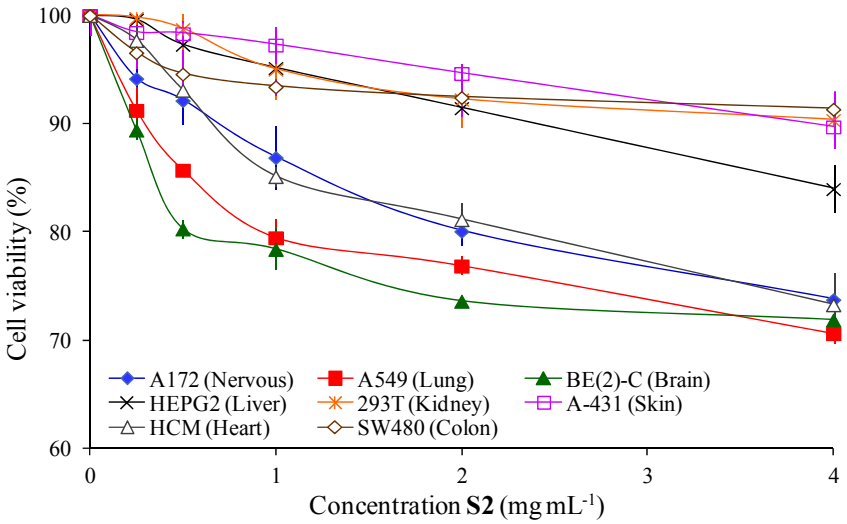

Figure SI-8. Cells viabilities of MTT assay results after 4 hours of treatment with various concentrations of solid **S2**.

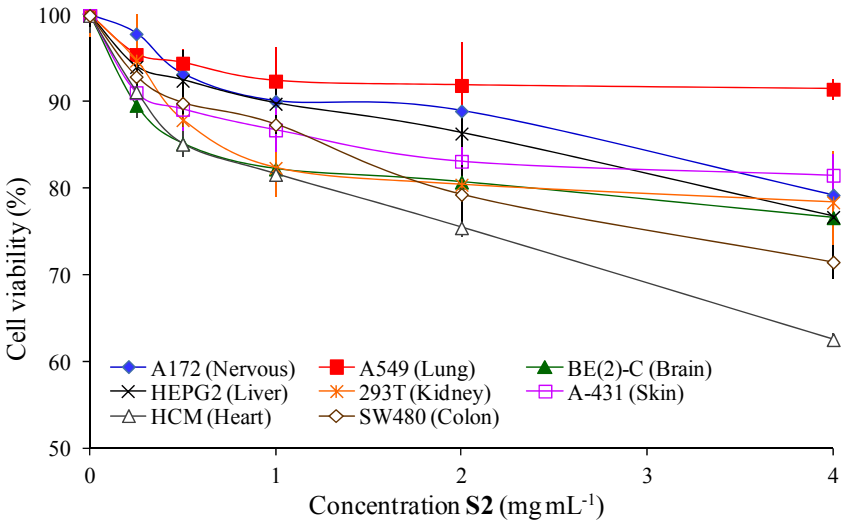

Figure SI-9. Cells viabilities of MTT assay results after 24 hours of treatment with various concentrations of solid **S2**.

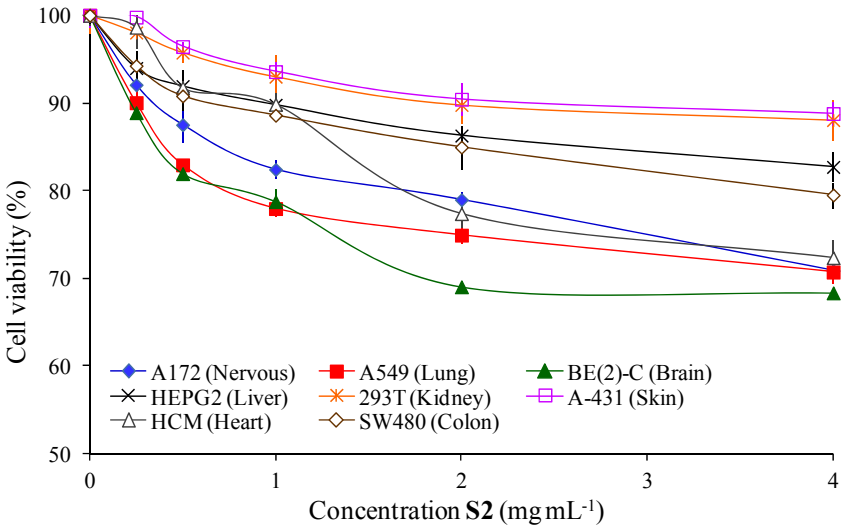

Figure SI-10. Cells viabilities of XTT assay results after 4 hours of treatment with various concentrations of solid **S2**.

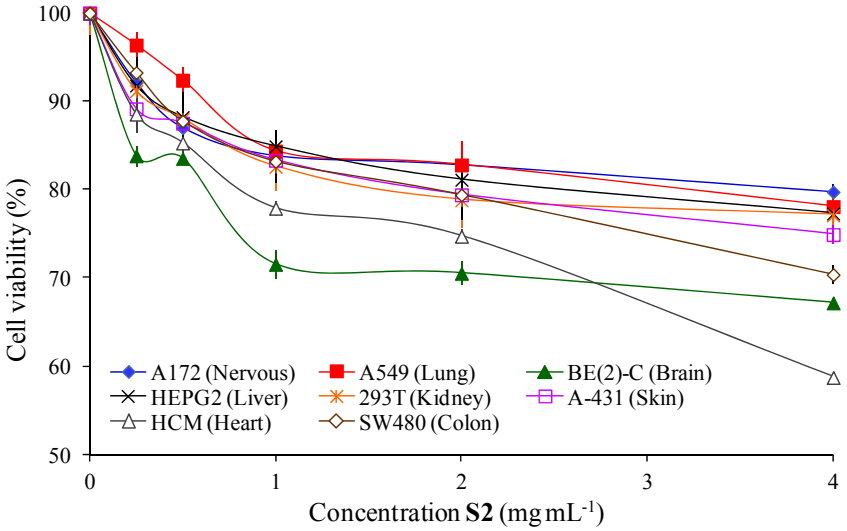

Figure SI-11. Cells viabilities of XTT assay results after 24 hours of treatment with various concentrations of solid **S2**.

b) Cell cycle assay

Cell cycle assays was carried out by staining of the DNA with Propidium Iodide (PI) followed by flow cytometric measurement of the fluorescence. Approximately 10^6 of K562 suspended leukemia cell line were maintained in culture after defreezing, to retain their physiologic cell cycle distribution. After achieving 75% confluence they were treated with the various amounts (0.25, 0.5, 1, 2, and 4 mg mL^{-1}) of solid **S2** for 24 hrs. The obtained suspensions of floating cells were centrifuged at 280 g. The collected cells were washed with PBS a couple of times at 200 g. The cells have been thoroughly resuspended in PBS by Pasteur pipette in order to have a monodisperse cell suspension at the time of

mixing cells with ethanol. Cells were fixed in ethanol via transferring into the tubes containing 70% ethanol and stored in -20°C for several days. Prior to the flow cytometric analysis, the ethanol-suspended cells were centrifuged at 300 g for 5 min and the supernatants were decanted thoroughly. The collected cells were washed with PBS and then suspended in 1 mL of PI/Triton X-100 staining solution with RNase A, followed by keeping at 37°C for 30 min. The stained cells were then analyzed by flow cytometry using Cyflow SL machine (Partec, Germany) with excitation at 488 nm and collecting data at FL2. The readings were analyzed with Flowjo software (Treestar Inc., CA, USA).

As shown in Figure SI-12 (a-f), solid **S2** did not show detectable effects on the cell-life cycle, even at high applied dosage (i.e. 4 mg mL^{-1}). More specifically, there were no traces of variations in apoptotic fraction (sub G_0G_1 stage), the G_0G_1 phase, S phase (i.e. DNA synthesis stage), and G_2M phase areas before and after interaction with NPs.

Cytotoxicity studies suggested that the silica NPs are completely biocompatible; however, for the targeted delivery of these particles to several sensitive organs (e.g. brain, lung, and heart), high concentration of NPs may cause the detectable trace of toxicities.

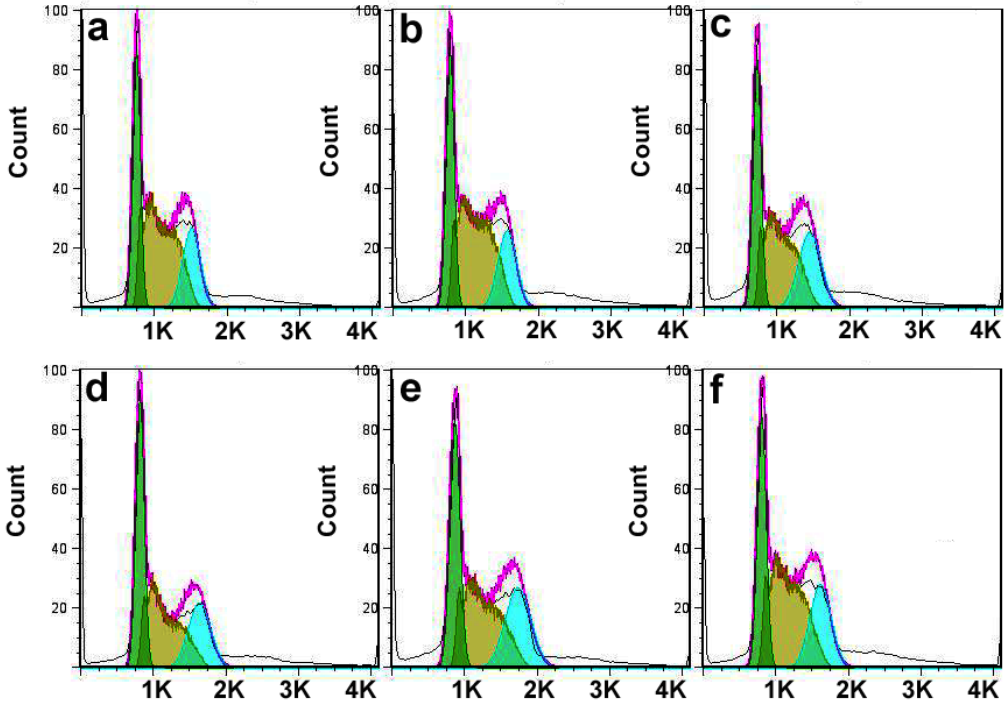

Figure SI-12. Cell-life cycle assay results for control (a) and (b)-(f) K562 cells exposed to different concentrations of solid **S2**: 0.25 mg mL^{-1} (b), 0.5 mg mL^{-1} (c), 1 mg mL^{-1} (d), 2 mg mL^{-1} (e), and 4 mg mL^{-1} (f).

Table of abbreviations

AC	Alternating current
AMF	Alternating magnetic field
ANOVA	Analysis of variance
CTAB	Hexadecyltrimethylammonium bromide
DI	Deionized
DMEM	Dubelcco's modified Eagle's medium
DNA	Deoxyribonucleic acid
DOPC	1,2-dioleoyl-sn-glycero-3-phosphocholine
EDS	Energy-dispersive X-ray spectroscopy
EDX	Energy-dispersive X-ray spectroscopy
FBS	Fetal bovine serum
MCM-41	Mobil's composition of matter-41
MTT	3-(4,5-dimethylthiazol-2-yl)-2,5-diphenyltetrazolium bromide
NP	Nanoparticle
PBS	Phosphate buffer saline
PI	Propidium iodide
PTFE	Polytetrafluoroethylene
RPMI	Roswell park memorial institute
SDS	Sodium dodecyl sulfate
SEM	Scanning electron microscopy
SPION	Superparamagnetic iron oxide nanoparticle
STEM	Scanning transmission electron microscopy
TEM	Transmission Electron Microscopy
TEOS	Tetraethylorthosillicate
TMAOH	Tetramethylammonium hydroxide
UV-vis	Ultraviolet-visible
VSM	Vibrating sample magnetometer
XRD	X-ray diffraction
XTT	Sodium (2,3-bis-(2-methoxy-4-nitro-5-sulphophenyl)-2H-tetrazolium-5-carboxianilide

Complete reference 8c

[8] c) C.E. Ashley, E.C. Carnes, G.K. Phillips, D. Padilla, P.N. Durfee, P.A. Brown, T.N. Hanna, J. Liu, B. Phillips, M.B. Carter, N.J. Carroll, X. Jiang, D.R. Dunphy, C.L Willman, D.N. Petsev, D.G. Evans, A.N. Parikh, B. Chackerian, W. Wharton, D.S. Peabody, *Nature Materials* 2011, **10**, 389.

References

(1) I.J. Bruce, J. Taylor, M. Todd, M.J. Davies E. Borioni, C. Sangregorio, T Sen, *J. Magnet. Magnet. Mater.* 2010, **284**, 145.

(2) L. Zhang, M.L. Longo, P. Stroeve, P. *Langmuir* 2000, **16**, 5093.

(3) T. Sen, A. Sebastianelli, I.J. Bruce, *J. Am. Chem. Soc.* 2006, **128**, 7130.

(4) T. Sen, G. Magdassi, G. Nizri, I.J. Bruce, *Micro & Nano Letters* 2006, **1**(1), 39.

(5) M. Ma, Y. Wu, J. Zhou, Y. Sun, Y. Zhang, N. Gu, *J. Magnet. Magnet. Mater.* 2004, **268**, 33.

(6) M. Mahmoudi, S. Laurent, M.A. Shokrgozar, M. Hosseinkhani, *ACS Nano*, 2011, **5**, 7263.

(7) M. Mahmoudi, K. Azadmanesh, M.A. Shokrgozar, W.S. Journeay, S. Laurent, *Chem. Rev.* 2011, **111**, 3407.

(8) V. Barnett, T. Lewis, John Wiley & Sons, 1994.